Molecular BioSystems

Accepted Manuscript

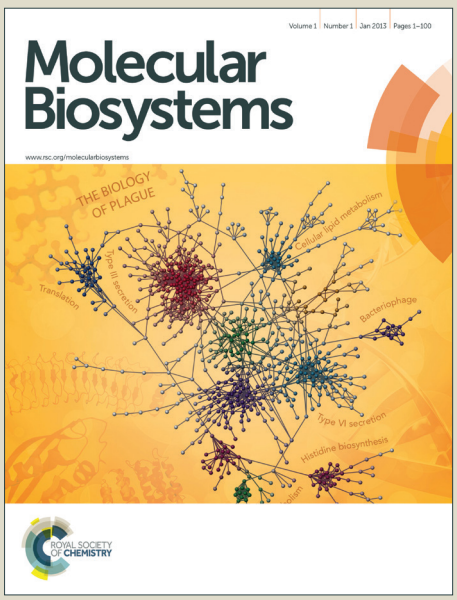

ROYAL SOCIETY OF CHEMISTRY

www.rsc.org/molecularbiosystems

Effect of Ru(II) polypyridyl complex $[Ru(bpy)_2(mdpz)]^{2+}$ on the stabilization of the RNA triplex poly(U)·poly(A)*poly(U)

Xiaojun He,[a] Jia Li,[a] Hong Zhao[a] and Lifeng Tan*[b]

[a] *College of Chemistry, Xiangtan University,* Xiangtan 411105, China

[b] *Key Lab of Environment-friendly Chemistry and Application in Ministry of Education, Xiangtan University, Xiangtan, China. E-mail: lfwyxh@yeah.net; lfwyxh@yahoo.com.cn. Fax: +86-731-5829-2251; Tel: +86-731-5829-3997*

There is renewed interest in investigating triplex nucleic acids because triplexes may be implicated in a range of cellular functions. However, the stabilization of triplex nucleic acids is essential to achieve their biological functions. In contrast to triplex DNA, little has been reported concerning the recognition of triplex RNA by transition-metal complexes at present. We report here a ruthenium(II) polypyridyl complex, $[Ru(bpy)_2(mdpz)]^{2+}$ (bpy = 2,2′-bipyridine; mdpz = 7,7'-methylenedioxyphenyl-dipyrido-[3,2-*a*:2',3'-*c*]phenazine) as a sensitive luminescent probe for poly(U)·poly(A)*poly(U), can strongly stabilize the triplex RNA from 37.5 to 53.1 ^{o}C in solution. The main results further advance our knowledge on the triplex RNA-binding by metal complexes, particularly ruthenium(II) complexes.

Introduction

Triplex nucleic acids, also called triplexes, are complexes of three oligonucleotide strands made

from either RNA or DNA.[1-3] Over the last decades, there is renewed interest in investigating triplex nucleic acids because triplexes may be implicated in a range of cellular functions, such as transcriptional regulation, post-transcriptional RNA processing and modification of chromatin.[4,5] However, the stability of triplexes is much lower than that of the corresponding duplex due to Hoogsteen base pairing, which hinders the possible applications of triple helices.[6–10] In this regard, small molecules able to recognize, bind and stabilize the specific sequences of the triple helical nucleic acid structures are of importance.

In recent years, many natural and synthetic small molecules able to stabilize triplex DNA under physiological conditions have been reported.[11–14] For example, neomycin as a groove binder, is the most effective aminoglycoside in stabilizing poly(T)•poly(A)*poly(T) (where •denotes the Watson-Crick base pairing and * denotes the Hoogsteen base pairing);[15] the natural polyamines and their analogs are also capable of stabilizing triplex DNA;[16,17] whereas the binding properties of $[Ru(II)(1,10\text{-phenanthroline})_2L]^{2+}$ complexes {where L is 1,10-phenanthroline (phen), dipyrido[3,2-*a*:2',3'-*c*]phenazine (dppz) or benzodipyrido[3,2-*a*:2',3'-*c*]phenazine (bdppz)} to poly(T)•poly(A)*poly(T) indicated that third-strand stabilization depended on the nature of the third substituted phenanthroline chelate ligand.[18] In contrast to triplex DNA, investigations on the stabilization of triplex RNA by small molecules are less well established, and studies at present are mainly focused on organic compounds[19–21] and, to a far lesser extent, on metal complexes.[22,23] In addition, previous reports indicate that stabilization of triplex RNA can be achieved by the action of intercalators,[24,25] in particular when covalently linked to the third strand.[26] However, intercalators not covalently linked can either stabilize or destabilize triplex RNA.[27,28] For example, the melting experiments suggest that ethidium,[29] proflavine (PR)[22] and its Pt-proflavine

complex (PtPR)[22] (Fig. 1) tend to destabilize the triplex, whereas some berberine analogs, such as BC1 [BC1 = 9–O–(*ω*-amino)–*n*-propyl–berberine] and BC2 [BC2 = 9–O–(*ω*-amino)–*n*-hexyl–berberine],[20] could strongly enhance the stabilization of the triplex RNA structure by intercalation. Interestingly, some alkaloids including their derivatives, such as coralyne, berberine and palmatine,[24] could stabilize the Hoogsteen base-paired third strand of the triplex almost without obvious affecting the stability of the duplex. These results reveal that small molecules effecting on the stabilization of triplex RNA are more complicated than previously thought.

We recently reported that the complex, $[Ru(bpy)_2(mdpz)]^{2+}$ (Ru**1**, Fig. 1; Ru = ruthenium; bpy = 2,2′-bipyridine; mdpz = 7,7'-methylenedioxyphenyl-dipyrido[3,2-*a*:2',3'-*c*]phenazine), bound to double-helical DNA with high affinity through intercalation and could act as a sensitive luminescent probe for DNA.[30] In light of the strong affinity of $[Ru(bpy)_2(mdpz)]^{2+}$ binding to DNA, in this paper we have investigated the interaction of this complex with poly(U).poly(A)*poly(U) to understand this complex effecting on the stabilization of poly(U)•poly(A)*poly(U) (Fig. 1).

Results and discussion

Emission titration

Luminescence measurement was first performed to determine the binding sensitivity of the Ru-complex to the RNA triplex. Fig. 2 shows the result when the fluorescence of Ru**1** is measured at 600 nm at different C_{UAU}/C_{Ru1} ratios {UAU stands for poly(U)·poly(A)*poly(U)}. Ru**1** shows negligible fluorescence in the absence of poly(U)•poly(A)*poly(U) in phosphate buffer solution at 20 ^{o}C (Fig. 2, red line). It can be reasonably surmised that hydrogen bonding and/or excited state proton transfer to the phenazine nitrogens as the mechanism of deactivation

of Ru**1**'s excited state, leading to Ru**1** showing weak fluorescence, similar to the well-known "DNA light switch" complex, $[Ru(bpy)_2(dppz)]^{2+}$ {dppz = dipyrido–[3,2–*a*:2',3'–*c*]phenazine}.[31,32] Upon first addition of the RNA triplex to Ru**1** (C_{UAU}/C_{Ru1} = 0.6), the fluorescence intensity of Ru**1** is instantly enhanced around 5 times than that of the initial intensity, which indicates that the fluorescence of Ru**1** is very sensitive to poly(U)•poly(A)*poly(U) and Ru**1** may act as a true and sensitive luminescent probe for poly(U)•poly(A)*poly(U). Upon continuous addition of the triplex RNA to the Ru**1**-UAU system, the fluorescence intensity increases gradually and finally an increase in fluorescence leads to a maximal of 28 times at C_{UAU}/C_{Ru1} = 15.0. This observation may imply that there is a strong and effective overlap between the aromatic surface of Ru**1** and the bases of poly(U)•poly(A)*poly(U) when Ru**1** binding to the triplex RNA. Therefore, it's difficult for Ru**1** to access water molecules in the presence of the RNA triplex, resulting in Ru**1** displaying more apparent fluorescence in comparison with Ru**1** alone.[33]

Electronic absorption spectral studies of the binding

Small molecules interact with triplex nucleic acids via a number of mechanisms, such as intercalation, groove binding and electrostatic interactions.[34] In general, small molecules with flat aromatic chromophore binding to triplexes usually results in hypochromism and bathchromism, due to the intercalation mode involving a π–π stacking interaction between the aromatic chromophore of the binding reagent and the base pairs of triplexes.[35] To investigate the possible binding modes of Ru**1** toward the triplex RNA, the interaction of Ru**1** with poly(U)•poly(A)*poly(U) has been further performed with UV-Vis absorption spectra. Changes in the spectral profiles during titration are shown in Fig. 3. The electronic absorption spectra of

Ru**1** alone is characterized by a metal to ligand charge-transfer (MLCT) transition band at 457 nm and two intraligand (IL) absorption bands at 288 and 395 nm, respectively. Upon the addition of poly(U)•poly(A)*poly(U), the MLCT and IL absorptions of Ru**1** exhibit significantly hypochromisms (*H*) although no obvious red shifts were observed (Table 1). The significantly hypochromisms reflect that a strong intermolecular interaction involving effective overlap of the π electron cloud of Ru**1** with the base triplets, which may result from Ru**1** intercalating into the base triplets.[23,24] In addition, both polarity effects of the triplex and electron transfer from the base triplets may also contribute to the spectral changes of Ru**1** to a certain extent. By fitting the absorption data[36] at 395 nm, the equilibrium binding constant, K_b, is estimated to be $(1.51 \pm 0.35) \times 10^6\ M^{-1}$, a similar order of magnitude to that reported for Ru**1** binding with double-helical DNA ($(2.1 \pm 0.1) \times 10^6\ M^{-1}$).[30] In addition, The binding constants K_b is smaller than that of so-called the triplex RNA-intercalative coralyne ($4.0 \times 10^6\ M^{-1}$),[24] but is more higher than those of the partial intercalation of PRPt[22] and alkaloid palmatine[24] to the RNA triplex {$1.3 \times 10^4\ M^{-1}$ for PtPR and $(8.0 \pm 0.30) \times 10^5\ M^{-1}$ for palmatine}. These indicate that the size and shape of small molecules have a significant effect on the binding affinities of small molecules toward the triplex RNA.

Determination of the binding mode by viscosity studies

To further clarify the binding mode of Ru**1** toward poly(U)•poly(A)*poly(U), viscosity measurements has been carried out by varying the C_{Ru}/C_{UAU} ratios. The effects of Ru**1** on the relative viscosity of poly(U)•poly(A)*poly(U) are presented in Fig. 4. The observed initial decrease in the relative specific viscosity of the RNA triplex at low concentrations may be indicative of a Ru**1**-induced conformational change in the triplex, whereas the subsequent increase in the solution viscosity may result from the effects of intercalation.[37] The initial

decrease in the apparent molecular length of the RNA triplex may be indicative of a conformational change in the triplex induced by Ru**1**, which may arise from the complex-induced kink or bend in the helix, thereby reducing the effective molecular length of the RNA triplex. In addition, the viscosity of the RNA triplex–Ru**1** system is different from that of the RNA triplex–PtPR.[22] Concerning the metal complex PtPR, only a partially intercalated complex can be formed due to the platinum-containing residues prevent full penetration of the PR residue between base planes. Thus, PtPR results in no obvious changes of the viscosity of poly(U)•poly(A)*poly(U). The results indicate that the binding mode of Ru**1** with poly(U)•poly(A)*poly(U) is intercalation and further suggest that the size and shape of metal complexes has a significant effect on the binding modes.

Conformational aspects of the binding

Conformational changes of the triplex RNA on binding of Ru**1** and Ru**2** was investigated by intrinsic circular dichroic studies. The intrinsic CD spectral pattern of poly(U)•poly(A)*poly(U) (Fig. 5) displays two distinct signals below 300 nm with a negative peak at about 240 nm and a positive peak at about 260 nm,[38] which may be attributed to the stacking interactions between the base triplets and the helical structure of the triplex strands. In addition, Ru**1** shows no intrinsic CD signals because it is a racemic compound. Therefore, any CD signals above 300 nm can be attributed to the interaction of Ru**1** with the RNA triplex, and below 300 nm, any changes from the RNA spectrum are due either to the RNA induced CD of the complex or the complex induced perturbation of the RNA spectrum.[39] Upon progressive addition of Ru**1** to the RNA triplex solution (Fig. 6), the conformation of the RNA triplex was found to be clearly perturbed with strong emergence of three new CD signals at 272, 302 and 456 nm, revealing that Ru**1** could bind

with the chiral environment of the RNA triplex with a strong interaction. Therefore, the result indicate that Ru**1** can induce the structural changes of the RNA triplex, which may be due to the intercalative ligand mdpz inserting deeply between the base pairs of the RNA triplex.[19]

Effect of Ru1 on the stabilization of the triplex RNA

A simple thermal melting experiment may be used to demonstrate the stabilization of a given structure by a small molecule.[40] In particular, with triplexes, the binding specificity of a small molecule toward the Hoogsteen base-paired third strand or to the Watson-Crick base-paired duplex can be very clearly discriminated.[40] In addition, the binding of a small molecule with nucleic acids may change the denaturation temperatures depending on the strength of its interactions with the different nucleic acid conformations.[18,35] The denaturation curves of poly(U)•poly(A)*poly(U) in the absence and presence of Ru**1** are presented in Fig. 7, and the quantitative data on the melting temperatures are summarized in Table 1. Ru**1**-free RNA melts in two well resolved sequential transitions: the first separation from the triplex occurs at about 37.5 ^{o}C (T_{m1}) corresponding to the dissociation of the RNA triplex to the poly(U)•poly(A) duplex and the poly(U) single strand, the second separation occurs at about 46 ^{o}C (T_{m2}) from the duplex strand separation, reflecting the denaturation of the remaining duplex poly(U)•poly(A) into its component single strands.[38] The melting experiments indicate that Ru**1** dose-dependently enhances the stabilization of the RNA triplex. Notably, Ru**1** could slightly increases the thermal stability of the RNA triplex at C_{Ru}/C_{UAU} below 0.08, whereas the stabilization of the RNA triplex registers remarkable enhancement at C_{Ru}/C_{UAU} above 0.08, while exerting a thermal stabilizing influence on the triplex at a C_{Ru}/C_{UAU} of 0.24 and stabilizes the Hoogsteen base paired third strand by about 15.6 ^{o}C. In addition, Ru**1** tends to destabilize the third strand poly(U) when the

ratios of C_{Ru}/C_{UAU} are above 0.24 (data not shown). Taken all these results together, the binding mode of Ru**1** to the RNA triplex is intercalation and Ru**1** binds more strongly toward the third strand poly(U) than the duplex poly(U)•poly(A) at the ratios of C_{Ru}/C_{UAU} are below 0.24. Furthermore, the above CD spectrum of poly(U)•poly(A)*poly(U) with Ru**1** also confirms that Ru**1** indeed stabilizes the triple helix.[23] In this case, we presume that that the main ligand mdpz of Ru**1** is intercalated with the two ancillary ligands bpy located in the minor groove of the triplex structure, thus stabilizing the third strand poly(U) by expansion of the stacking interaction. In addition, the cationic nature of Ru**1** account for at least part of the triplex stabilization. Notably, the effect of Ru**1** on the stabilization of poly(U)•poly(A)*poly(U) is obviously different from some alkaloids[24], ethidium,[29] proflavine and its metal complex PtPR.[38] The previous investigations show that, ethidium, proflavine and its metal complex, tend to destabilize the Hoogsteen base-paired third strand poly(U) and to stabilize the duplex poly(U)•poly(A) of poly(U)•poly(A)*poly(U), whereas some alkaloids, such as berberine, palmatine and coralyne, can stabilize the Hoogsteen base-paired third strand of the triplex with no obvious affecting on the stability of the duplex. More recently, the mechanisms of the binding of coralyne toward poly(U).poly(A)*poly(U) indicate that coralyne is able to induce the triplex-to-duplex conversion and also the duplex-to-triplex conversion,[40] which may explain why coralyne tend to stabilize the triplex. These reveal that the effects of small molecules on the stability of the triplex RNA are very complicated and sensitive to their structural features and interaction processes.

Conclusions

The interaction of Ru**1** with the RNA triplex poly(U).poly(A)*poly(U) has been studied by various biophysical techniques. Results obtained here indicate that Ru**1** may act as a sensitive luminescent probe for poly(U)·poly(A)*poly(U) in solution and can obviously stabilize the Hoogsteen base-paired third strand of the triplex. This study further advance our knowledge on the triplex RNA-binding by metal complexes, particularly ruthenium(II) complexes. Future studies will aim to determine the exact mechanisms of action between Ru**1** and the triplex RNA.

Experimental section

Materials

Polynucleotide samples of double stranded poly(A)•poly(U) and single stranded poly(U) were obtained from Sigma-Aldrich Corporation (St. Louis, MO, USA) and were used as received. Poly(U)·poly(A)*poly(U)[23] and Ru**1**[30] were prepared as reported earlier. The concentration of poly(U)·poly(A)*poly(U) was determined optically using molar extinction coefficients, ε (M^{-1} cm^{-1}) reported in the literature.[24,38,41] All titration experiments were conducted at 20 °C in pH 7.0 phosphate buffer (6 mmol/L Na_2HPO_4, 2 mmol/L NaH_2PO_4, 1 mmol/L Na_2EDTA, 19 mmol/L NaC1).

Apparatus and measurements

Emission titration. Emission titrations was carried out on a Perkin Elmer LS-55 luminescence spectrometer, and a dilute solution of Ru**1** (2 uM) in phosphate buffer was excited at 470 nm. After each addition, the solution was mixed and allowed to re-equilibrate for at least 5 min before recording the curve. For all titrations, a small increase in the final volume (< 3%) of the sample occurred.

Electronic absorption spectral studies of the binding. UV-vis spectra were collected using a Perkin-Elmer Lambda-25 spectrophotometer at 20 °C. A typical titration of Ru**1** in phosphate buffer was performed by using a fixed Ru**1** concentration, to which the RNA triplex stock solution was gradually added up to saturation. After each addition, the solution should be mixed and allowed to re-equilibrate for at least 5 min before recording the absorption spectra. The intrinsic binding constant K_b and the binding site s of Ru**1** to the triplex RNA from absorbance titrations are calculated by using the following equation.[36]

$$\frac{\varepsilon_a - \varepsilon_f}{\varepsilon_b - \varepsilon_f} = \frac{\sqrt{b - (b^2 - 2K_b^2 C_t[RNA]/s)}}{2K_b C_t} \quad (1a)$$

$$b = 1 + K_b C_t + K_b[RNA]/(2s) \quad (1b)$$

where [RNA] is the concentration of poly(U)·poly(A)*poly(U) in the nucleotide phosphate and ε_a, ε_f and ε_b are the apparent, free and bound metal complex extinction coefficients, respectively. K_b is the equilibrium binding constant in M^{-1}, C_t is the total metal complex concentration and s is the average binding size. When plotting $(\varepsilon_a - \varepsilon_b)/(\varepsilon_f - \varepsilon_b)$ *vs.* [RNA], K_b is given by the ratio of the slope to the intercept.

Determination of the binding mode by viscosity studies. Viscosity measurements were carried out using an Ubbelodhe viscometer maintained at a constant temperature of (20 ± 0.1) °C in a thermostatic bath. The flow time was measured with a digital stopwatch, and each sample was tested by three times to get an average calculated time. Relative viscosities for the triplex RNA either in presence or absence of Ru(II) complexes were calculated as reported earlier.[41] The relative increase in length, L/L_0, may be obtained from the corresponding increase in relative

viscosity with the use of the equation, $\frac{L}{L_0} = (\frac{\eta}{\eta_0})^{\frac{1}{3}}$, where L and L_0 are the contour lengths of triplex in the presence and absence of Ru(II) complexes, η is the viscosity of RNA in the presence of Ru(II) complexes, η_0 is the viscosity of RNA alone.

Conformational aspects of the binding. Circular dichroic spectrum of the RNA triplex in the absence of Ru**1** was performed with a Jasco-810 spectropolarimeter equipped with a thermoelectric cell temperature controller (model PFD 425S). A rectangular strain-free quartz cell of 1 cm path length was used. The CD spectra of the RNA triplex in the presence of the complex was recorded in phosphate buffer at 20 ^{o}C. After each addition of Ru**1**, the solution was mixed and allowed to re-equilibrate for at least 5 min before recording the CD spectra. Each spectrum was averaged from three successive accumulations and was baseline-corrected, smoothed and normalized to nucleotide phosphate concentration in the region 200-500 nm using the software supplied by Jasco. The molar ellipticity (θ) values are expressed in deg·cm^2 dmol$^-$

Effect of Ru1 on the stabilization of the triplex RNA. Thermal RNA denaturation experiments were carried out with a Perkin-Elmer Lambda-25 spectrophotometer equipped with a Peltier temperature-control programmer (± 0.1 ^{o}C). The temperature of the solution was increased from 20 to 65 ^{o}C at a rate of 0.5 or 1.0 ^{o}C min^{-1}, and the absorbance at 260 nm was continuously monitored for solutions of the RNA Triplex (30 μM) in the presence of different concentrations of Ru**1**. The data were presented as $(A - A_0)/(A_f - A_0)$ versus T (T = temperature}, where A_f, A_0, and A are the final, the initial, and the observed absorbance at 260 nm, respectively. The T_m value (T_m is defined as the temperature of melting) is obtained from the first derivative curve ($d\alpha/dT$) ($\alpha = (A - A_0)/(A_f - A_0)$), and the manual curves gave identical values.

Acknowledgements

This work was supported by the National Natural Science Foundation of China (21071120 and 21371146), Hunan Provincial Natural Science Foundation of China (12JJ2011) and the Key Project of Chinese Ministry of Education (212127).

Referencrs

1 G. Felsenfeld, D. R. Davies and A. Rich, *J. Am. Chem. Soc.,* 1957, *79*, 2023–2024.

2 H. E. Moser and P. B. Dervan, *Science,* 1987, 238, 645–650.

3 T. L. Doan, L. Perrouault, M. Chassignol, T. T. Nguyen, C. S. Hélène, *Nucleic Acids Res.,* 1987, 15, 8643–8659.

4 A. Jain, A. Bacolla, P. Chakraborty, F. Grosse and K.M. Vasquez, *Biochemistry,* 2011, *49*, 6992–6999.

5 N. K. Conrad, *Wiley Interdiscip Rev. RNA*., 2014, 5, 15–29.

6 A. C. Laura, A. F. Rick and J. B. Adam, *Cancer Res*., 2006, 66, 4089−4094.

7 M. Li, T. Zengeya and E. Rozners, *J. Am. Chem. Soc*., 2010, 132, 8676−8681.

9 A. F. Buske, J. S. Mattick, T. L. Bailey, *RNA Biol*., 2011, 8, 427−439.

10 P. Gupta, O. Muse and E. Rozners, *Biochemistry,* 2012, 51, 63–73.

11 A. Nadal, R. Eritja, T. Esteve and M. Pla, *Chembiochem,* 2005, 6, 1034–1042.

12 G. N. Ben, Z. Zhao, S. R. Gerrard, K. R. Fox and T. Brown *Chembiochem,* 2009, 10, 1839–851.

13 O. Doluca, A.S. Boutorine and V.V. Filichev, *Chembiochem,* 2011, 12, 2365–2374.

14 D. Bhowmik and G. S. Kumar *Mol. Biol. Rep.*, 2013, 40, 5439–5450.

15 D. P. Arya, L. Micovic, I. Charles, R. Lane Coffee, J. B.Willis and L. Xue, *J. Am. Chem. Soc.,*

2003, 125, 3733–3744

16 T. Thomas and T. J. Thomas, *Biochemistry,* 1993, 32, 14068–14074.

17 M. Musso, T. Thomas, A. Shirahata, L. H. Sigal, M. W. Van Dyke and T. J. Thomas, *Biochemistry,* 1997, 36, 1441–1449

18 S. D. Choi, M. S. Kim, S. K. Kim, P. Lincoln, E. Tuite and B. Nordén, *Biochemistry,* 1997, 36, 214–223

19 D. P. Arya, *Acc. Chem. Res.* 2011, 44, 134–146.

20 D. Bhowmik, S. Das, M. Hossain, L. Haq and G. S. Kumar, *PLoS ONE,* 2012, 7, e37939–e37939.

21 H. J. Lozano, B. García, N. Busto and J. M. Leal *J. Phys. Chem., B.* 2013, 117, 38–48.

22 B. García, J. M. Leal, V. Paiotta, R. Ruiz, F. Secco and M. Venturini, *J. Phys. Chem. B.,* 2008, 112, 7132–7139.

23 L. F. Tan, J. Liu, J. L. Shen, X. H. Liu, L. L. Zen and L. H. Jin, *Inorg. Chem.,* 2012, 51, 4417–4419.

24 R. Sinha and G.S. Kumar, *J. Phys. Chem. B.,* 2009, 113, 13410–13420.

25 H. J. Xi, E. Davis, N. Ranjan, L. Xue, D. Hyde-Volpe and D.P. Arya, *Biochemistry,* 2011, 50, 9088–91113.

26 A. K. Shchyolkina, E. N. Timofeev, Y. P. Lysov, V. L. Florentiev, T. M. Jovin and D. J. Arndt-Jovin, *Nucleic Acids Res.,* 2001, 29, 986–995.

27 M. Polak and N. V. Hud, *Nucleic Acids Res.*, 2002, 30, 983–992.

28 E. A. Lehrman and D. M. Crothers, *Nucleic Acids Res.,* 1977, 4, 1381–1392.

29 B. Garcia, J. M. Leal, V. Paiotta, S. Ibeas, R. Ruiz, F. Secco and M. Venturini, *J. Phys. Chem. B.,* 2006, 110, 16131–16138.

30 L. F. Tan, H. Chao, J. J. Fei, G.J. Su, S. Zhang and Y. Xia, L. N. Ji, *Aust. J. Chem.,* 2008, 61, 376–381.

31 A. E. Friedman, J. C. Chambron, J. P. Sauvage,N. J.Turro and J. K. Barton, *J. Am. Chem. Soc.,* 1990, 112, 4960–4962.

32 E. J. C. Olson, D. Hu, A. Hormann, A. M. Jonkman, M. R. Arkin, E. D. A. Stemp, J. K. Barton and P. F. Barbara, *J. Am. Chem. Soc.,* 1997, 119, 11458–11467.

33 S. Shi, J. Zhao, X. T. Geng, T. M. Yao, H. L. Huang, T. L. Liu, L. F. Zheng, Z. H. Li, D. J. Yang and L. N. Ji, *Dalton Trans.,* 2010, 39, 2490–2493.

34 T. Biver, *Coord. Chem. Rev.,* 2013, 257, 2765– 2783.

35 A. Kabir and G. S. Kumar, *Mol. BioSyst.,* 2014, 10, 1172–1183.

36 M.T. Carter, M. Rodriguez and A.J. Bard, *J. Am. Chem. Soc.,* 1989, *111*, 8901–8911.

37 P. V. Scaria and R. H. Shafer, *J. Biol. Chem.*, 1991, 266, 5417–5423.

38 S. Das, G. S. Kumar, A. Ray and M. Maiti, *J. Biomol. Struct. Dyn.,* 2003, *20*, 703–714.

39 B. Tijana, N. Olga, H. Anna, Z. Lenka, V. Oldrich, K. Jana, H. Abraha, P. Simon, J. S. Peter and B. Viktor, *J. Med. Chem.,* 2008, 51, 5310–5319.

40 F. J. Hoyuelos, B. García, J. M. Leal, N. Busto, T. Biver, F. Secco and M. Venturinib, *Phys. Chem. Chem. Phys.,* 2014, 16, 6012–6018.

41 G. Cohen, H. Eisenberg, *Biopolymers,* 1969, *8*, 4549–4560.

Captions for Figures

Fig. 1 Chemical structures of proflavine (PR), Pt-proflavine complex (PtPR), Ru**1** and the base pairing scheme in poly(U)•poly(A)*poly(U) (where •denotes the Watson-Crick base pairing and * denotes the Hoogsteen base pairing).

Fig. 2 Representative fluorescence emission spectra of Ru**1** (2.0 uM) treated with poly(U)·poly(A)*poly(U) in phosphate buffer (6 mmol/L Na_2HPO_4, 2 mmol/L NaH_2PO_4, 1 mmol/L Na_2EDTA, 19 mmol/L NaC1, pH 7.0) at 20 ^oC. [UAU] = 0–30 μM {UAU stand for poly(U)·poly(A)*poly(U)}. The arrow show the absorbance change upon an increasing poly(U)·poly(A)*poly(U) concentrations. Inset: plots of I/I_0 versus [UAU]/[Ru], where I_0 and I are the fluorescence intensities in the absence and presence of poly(U)·poly(A)*poly(U).

Fig. 3 Representative absorption spectral changes of Ru**1** (20 μM) in the presence of poly(U)•poly(A)*poly(U) in phosphate buffer at 20 ^oC. [UAU] = 0–36.3 μM. The arrows show the absorbance change upon an increasing poly(U)·poly(A)*poly(U) concentrations. Inset: plots of plotting $(\varepsilon_a - \varepsilon_b)/(\varepsilon_f - \varepsilon_b)$ *vs.* [UAU] and the nonlinear fit. Solution conditions are the same as those described in the legend of Fig. 2.

Fig. 4 Viscometric Ru**1** titrations of poly(U)•poly(A)*poly(U) (153 μM) in phosphate buffer at 20 ^oC. Solution conditions are the same as those described in the legend of Fig. 2.

Fig. 5 Circular dichroic spectra of poly(U)•poly(A)*poly(U) (30.0 Mm, A) treated with Ru**1** (B) in phosphate buffer at 20 ^oC. Solution conditions are the same as those described in the legend of Fig. 2. The arrows show CD signal changes upon an increasing Ru**1** concentrations.

Fig. 6 Melting curves of poly(U)•poly(A)*poly(U) (30 μM) in the absence and prescence of Ru**1** at different [Ru**1**]/[UAU] ratios. Solution conditions are the same as those described in the legend of Fig. 2.

Table 1 Binding constants (K_b), average binding site size (s), hypochromicity ($H\%$) and bathochromic shifts of Ru**1**.

Title	$\lambda_{max,\ free}$ (nm)	$\lambda_{max,\ bound}$ (nm)	$\Delta\lambda^a$ (nm)	H^b (%)	$K_b{}^c$ ($\times 10^6\ M^{-1}$)	S^d
Ru**1**	288	270	2	20.5	–	–
	395	398	3	32.2	7.51 ± 0.89	2.54 ± 0.07
	457	457	0	18.8	–	–

[a] $\Delta\lambda$ represents the difference in wavelength of the IL and MLCT band of the metal complex between free and completely bound DNA states. [b] $H\% = (A_{free} - A_{bound})/A_{free.}\ 100\%$ (A is the absorbance). [c] K_b was determined by monitoring the changes of absorption at the IL band at 392 nm. [d] s is an average binding size.

Table 1 Melting Temperature (°C) for poly(U)•poly(A)*poly(U) in the absence and presence of Ru**1**; [Na^+] = 35 mM. T_{m1} and T_{m2} correspond to triplex to duplex and duplex to single strand transitions, respectively. ΔT_m = [T_m of triplex-Ru**1** - T_m of triplex].

Title/Complex	C_{Ru}/C_{UAU}	T_{m1} (°C)	T_{m2} (°C)	ΔT_{m1}	ΔT_{m2}
poly(U)•poly(A)*poly(U)	0	37.5	46.0	–	–
poly(U)•poly(A)*poly(U) + Ru**1**	0.01	40.0	50.2	3.5	4.2
	0.05	41.2	50.5	3.7	4.5
	0.08	41.5	51.0	4.0	5.0
	0.12	46.0	52.5	8.5	6.5
	0.16	51.7	–	14.2	–
	0.20	52.0	–	14.5	–
	0.24	53.1	–	15.6	–

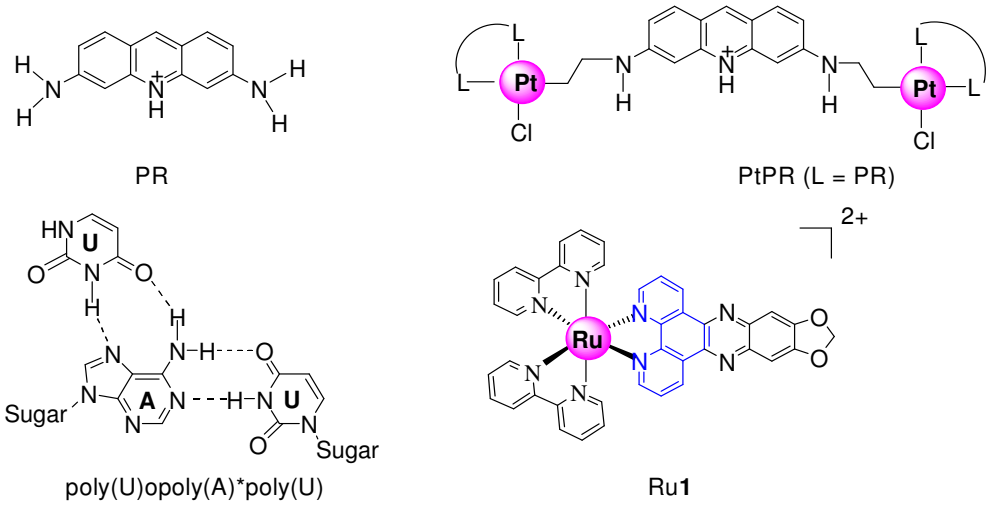

Fig. 1

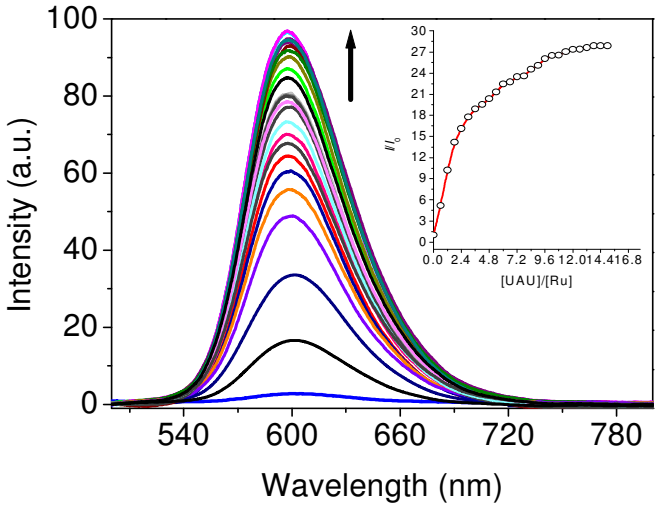

Fig. 2

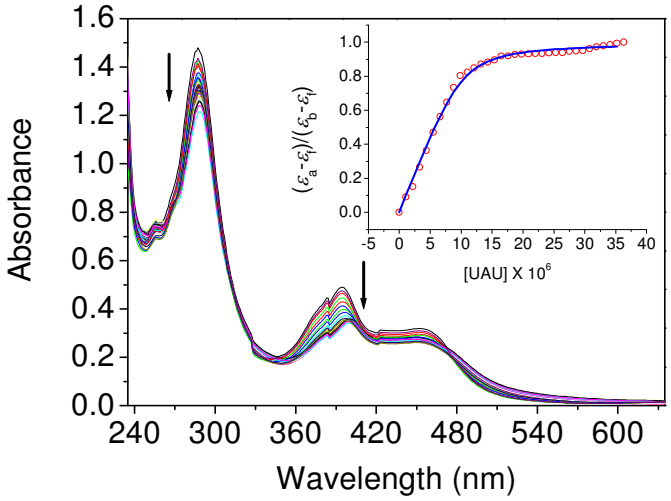

Fig. 3

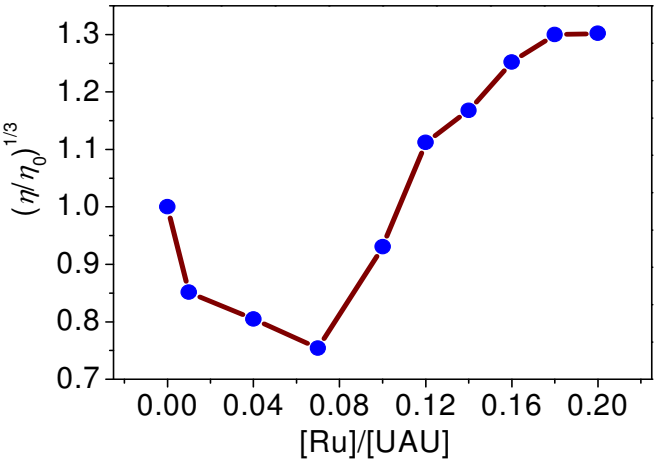

Fig. 4

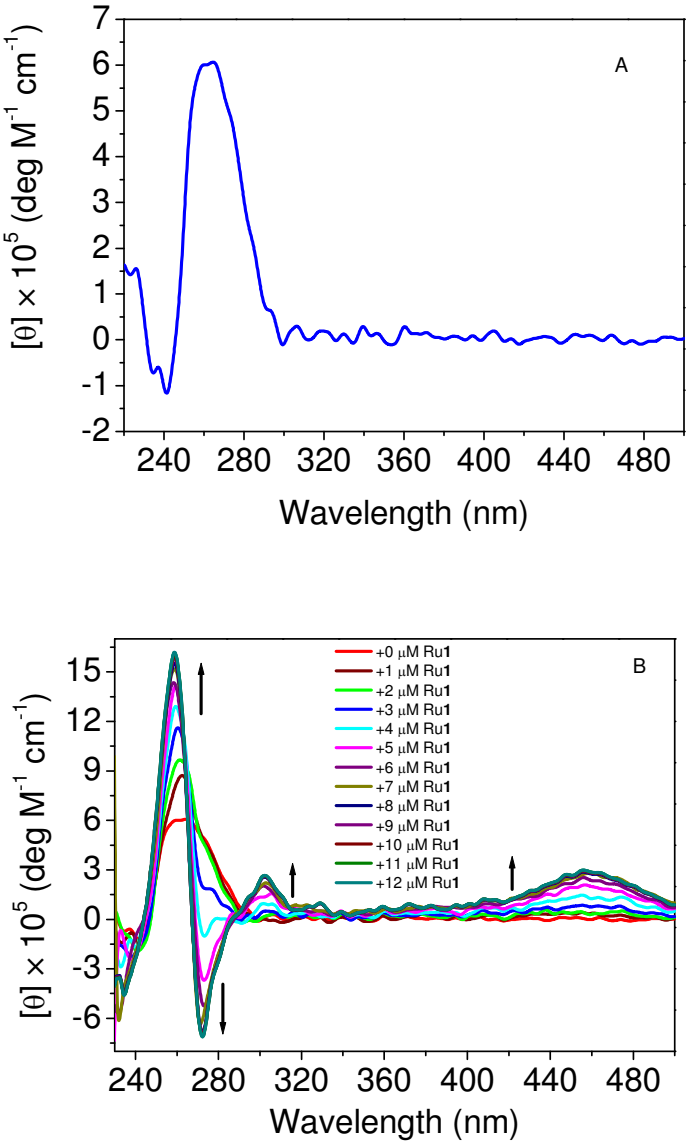

Fig. 5

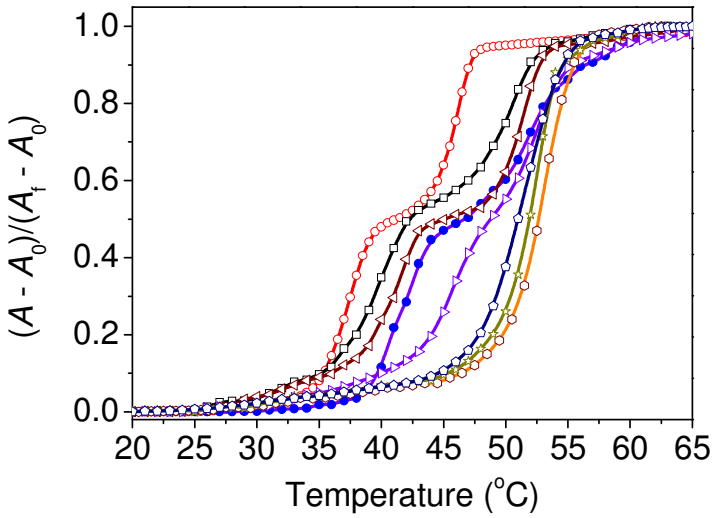

Fig. 6